Pain peptides. Solution structure of orphanin FQ2

Pietro Amodeo[a], Blanca López Méndez[a,b], Remo Guerrini[c], Severo Salvadori[c], Piero A. Temussi[d], Teodorico Tancredi[a,*]

[a] *Istituto di Chimica MIB, CNR, Via Toiano 6, Arco Felice, I-80072 Naples, Italy*
[b] *Departamento de Química Orgánica, Facultad de Química e Instituto de Acuicultura, Universidad de Santiago de Compostela, E-15706 Santiago de Compostela, Spain*
[c] *Dipartimento di Scienze Farmaceutiche, Università di Ferrara, Via Fossato di Mortara 17/19, I-44100 Ferrara, Italy*
[d] *Dipartimento di Chimica, Università di Napoli Federico II, Via Mezzocannone 4, I-80134 Naples, Italy*

Received 22 February 2000; received in revised form 7 April 2000

Edited by Pierre Jolles

Abstract Orphanin FQ2 (OFQ2) is a novel heptadecapeptide generated from prepronociceptin (PPNOC), the same precursor of nociceptin/orphanin FQ and nocistatin. OFQ2 is a potent analgesic when administered both supraspinally and spinally. In order to clarify the structural relationship with all peptides generated from PPNOC, we have undertaken the conformational study of OFQ2 in water and in structure-promoting solvent media. Nuclear magnetic resonance data and theoretical calculations are consistent with a well defined helical structure from Met[5] to Ser[16]. The uniform distribution of hydrophobic residues along the helix suggests that OFQ2 may interact with the transmembrane helices of a receptor akin to those of nociceptin and opioids.

Key words: Nociception; Bioactive peptide; Opioid; Conformation; Nuclear magnetic resonance

1. Introduction

Nociceptin/orphanin FQ (FGGFTGARKSARKLANQ, henceforth called NC) and orphanin FQ2 (FSEFMRQYLVLSMQSSQ) (OFQ2) are two biologically active heptadecapeptides processed from the same precursor, prepronociceptin (PPNOC) [1–3]. Both have an N-terminal sequence characterized by two aromatic residues spaced by two residues reminiscent of the message domain of the well known opioid heptadecapeptide dynorphin A (YGGF). Recently, it has been reported [3] that bovine PPNOC contains another biologically active heptadecapeptide named nocistatin. Bovine nocistatin, TEPGLEEVGEIEQKQLQ, plays a role opposite to that of nociceptin in pain transmission but it is not related in any obvious way to known opioid peptides. Both the sequence of the message domain and the conformational behavior suggest a structure–activity relationship different from those of dynorphin A and nociceptin. In opioids and nociceptin, the message domains are the N-terminal part (YGGF and FGGF, respectively), whereas the shortest fragment of nocistatin that retains allodynia-blocking activity is the C-terminal hexapeptide (EQKQLQ), which is conserved in bovine, human and murine species. Dynorphin A [4] and nociceptin [5] show little tendency to form well defined structures in solution, not only in water and other polar solvents, but also in helix-inducing media. Nocistatin, on the other hand, forms a well defined structure extending from Gly[4] to Leu[16], with an unusually well defined helix (for a short peptide) in the C-terminal part [6].

NC is an endogenous ligand for the opioid receptor-like 1 (ORL1). Activation of this receptor by NC involves many physiological functions, both in the periphery and in the central nervous system [7,8]; in particular, NC evokes hyperalgesia and anti-opioid effects in the brain and analgesia in the spinal cord [9]. Nocistatin blocks NC-induced allodynia and hyperalgesia and attenuates pain evoked by prostaglandin E2 [3]. OFQ2 was tested for its ability to activate or to bind to the ORL1 receptor expressed in CHO cells and in mouse brain homogenates. It was found unable to displace ^{125}I-Tyr[14]-NC binding on membranes of ORL1 receptor-transfected CHO cells and to induce an inhibition of forskolin-stimulated cAMP at concentrations up to 10 μM [5]. In competition binding studies, OFQ2 showed IC_{50} values larger than 1 μM against all the traditional opioid receptors and did not compete with NC–radioligand binding in mouse brain homogenates [5]. However, Pasternak et al. [12] reported that OFQ2 is a potent analgesic given either supraspinally or spinally, and while supraspinal OFQ2 analgesia is readily reversed by naloxone, implying activation of opioid receptor systems, spinal OFQ2 analgesia is insensitive to opioid antagonists. Moreover, the existence of a specific receptor for OFQ2 has recently been demonstrated by Florin et al. [11].

The differences in biological role, together with the mentioned conformational preferences of dynorphin A [4], NC [5] and nocistatin [6] prompted a detailed conformational study of OFQ2. Determination of the conformational state in solution of the OFQ2 may shed light on the proposed role of this new peptide in pain transmission and on the type of interaction with different hitherto unknown receptors. OFQ2 was thus studied in solution conditions similar to those employed for the other PPNOC peptides. The best structuring conditions were found in hexafluoroacetone trihydrate (HFA)/water (50:50, v/v) at 300 K.

2. Materials and methods

2.1. Peptide synthesis and analytical determinations

OFQ2 was synthesized according to published methods using standard solid-phase synthesis techniques [12]. Protected amino acids and chemicals were purchased from Bachem, Novabiochem or Fluka (Switzerland). The resin (4-hydroxymethylphenoxyacetic acid) on the polyethyleneglycol/polystyrene support, loaded with N^{α}-Fmoc-N^{γ}-(Trt)-Gln (Fmoc-Gln(Trt)-PAC-PEG-PS) was from Millipore

*Corresponding author. Fax: (39)-81-8534236.
E-mail: ttancredi@icmib.na.cnr.it

PII: S0014-5793(00)01513-1

(Waltham, MA, USA). The protected peptide–resin was treated with trifluoroacetic acid (TFA)/water/triethylsilane 88/5/7 (10 ml/0.2 g of resin) for 1 h at room temperature, crude peptide was purified by preparative reversed-phase high performance liquid chromatography (HPLC) on a column C_{18} (30×4 cm, 300 Å, 15 μm spherical particle size) perfused at a flow rate of 40 ml/min with a mobile phase containing solvent A (10%, v/v, acetonitrile in 0.1% TFA), and a linear gradient from 10 to 60% of solvent B (60%, v/v, acetonitrile in 0.1% TFA).

Analytical HPLC analyses were performed on a Alltech column C_{18} (4.6×150 mm, 5 μm particle size) using the above solvent system programmed at a flow rate of 1 ml/min with a linear gradient from 0% to 80% B in 25 min.

Molecular weights of the compounds were determined by a matrix-assisted laser desorption ionization time of flight analysis using a Hewlett Packard G2025A LD-TOF system mass spectrometer and α-cyano-4-hydroxycinnamic acid as a matrix.

2.2. Nuclear magnetic resonance (NMR) experiments

NMR sample was prepared by dissolving appropriate amounts of peptide in 0.5 ml of solvents to make approximately 2 mM solutions. All spectra were run at 300 K on a Bruker DRX-500 instrument, operating at 500 MHz for ^{1}H. All chemical shifts, in parts per million, are referred to the methyl resonance of TMS or TSP. One dimensional NMR spectra were acquired using 32 scans with 32k data size. Two dimensional TOCSY [13] and NOESY [14] spectra were recorded by using the time-proportional phase incrementation of the first pulse [15], with water suppression by presaturation. A TOCSY spectrum was collected with a mixing time of 50 ms, using the clean MLEV-17 mixing scheme [13]. NOESY spectra were recorded with mixing times of 80, 100 and 120 ms. Data processing and analysis were performed with standard Bruker software (XwinNMR, AURELIA) and NMRView [16].

2.3. Structure calculations

NOESY cross-peaks from 100 ms spectrum were integrated using NMRView and translated into interatomic distances using CALIBA, a routine of DYANA [17]. The structure calculations were performed using both DYANA and the AMBER 5.0 package [18].

2.3.1. Structure calculations with AMBER 5.0. The calculations were performed using the AMBER all-atom 1991 parameterization, with a distance dependent dielectric constant $\varepsilon = r_{ij}$, and a cutoff radius of 8 Å for non-bonded interactions. Two sets of initial structures were generated, using the standard residue charges and reduced net charges (±0.2 atomic units) on charged residues, respectively. This second set is useful for in vacuo simulations, in order to compensate in part for neglect of explicit solvent. Energy minimizations (EM) were performed by a combination of steepest descent and conjugate gradient algorithms, to a gradient norm of 10^{-4} kcal/mol/Å.

Each set of EM initial structures underwent two different multiple restrained simulated annealings (SA). In both cases, SA cycles of five runs of 50 000 molecular dynamics (MD) steps were run, but a shorter time step was chosen (0.0015 vs. 0.0020 ps) in higher maximum temperature (1200 K) runs. Distance restraints were applied by a square bottom with parabolic sides penalty function, and a force constant of 20 kcal/mol/Å. Data were collected each 500 steps for analysis. 50 periodically selected structures were chosen from each SA cycle, and minimized to represent the solution structure.

2.3.2. Structure calculations with DYANA. A set of structures was generated by DYANA [17] by torsion angle dynamics. A total of 60 structures were calculated by SA, starting with a total of 4000 MD steps and default values of temperature and time steps. The best 50 structures in terms of target function were refined by EM with the SANDER module of AMBER 5.0 and selected to represent the solution structure. All the structures were analyzed with the program MOLMOL [19], also used to plot Figs. 3 and 4a,b.

3. Results

OFQ2 is virtually insoluble in water and neat DMSO and has a very small solubility in a mixture of water with DMSO. Spectra of OFQ2 in the DMSO/water cryomixture, however, are not of sufficient quality to yield detailed structural information. On the contrary, media that are known to favor helical conformations show NOESY spectra consistent with a high helical content. Alcohols, either neat or mixed with water, have often been used to induce helicity in peptides [20]. We ran spectra of OFQ2 in mixtures of water with TFE and HFA. This last mixture has recently been shown to behave like TFE/water mixtures but with a much higher helix-inducing propensity [21]. We have also shown that the structuring effect of HFA/water, although very strong, reflects intrinsic residue tendencies faithfully. In fact, it is possible to observe structured and unstructured tracts in the same peptide dissolved in HFA/water. For instance, β-endorphin, another long-chain opioid, in HFA/water assumes a regular helical structure only in the C-terminal address domain sequence, leaving the first 12 residues completely disordered [22].

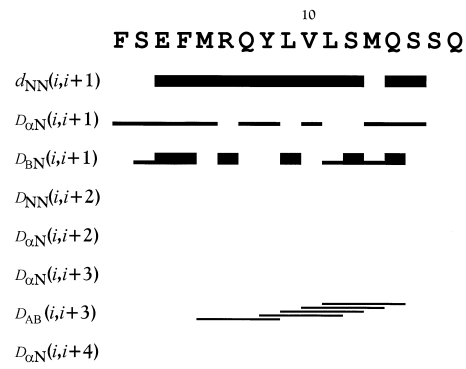

Fig. 1. Diagrammatic representation of sequential and secondary structural interresidue NOEs ($\tau_m = 100$ ms) observed for OFQ2 in HFA/water (50% v/v) at 300 K.

Assignment of proton spin systems was obtained with the sequential methodology. In the NH–NH region of a NOESY spectrum, it is possible to follow the connectivities from Glu^3 to Ser^{16} with only few interruptions due to cross-peak overlap in the region from Leu^{11} to Gln^{14}. Several attempts to eliminate this overlap, either running spectra at different temperatures or solvent mixtures (e.g. DMSO/water), were unsuccessful. The solution structure of OFQ2 was delineated from quantitative analysis of the sequential and medium-range NOEs. Fig. 1 shows the summary of diagnostic NOEs in HFA/water at 300 K and 100 ms mixing time. The strong NH_i–NH_{i+1} NOEs (from Glu^3 to Ser^{16}) and the corresponding weaker $C_\alpha H_i$–NH_{i+1} NOEs are features typical of helical structures. The observations of several unambiguous medium-range NOEs, from Met^5 to Gln^{14}, are also in favor of the presence of an helix in this peptide region. Distance restraints deriving from intraresidue, sequential and medium-range NOEs were introduced in SA calculations performed with both AMBER 5.0 and DYANA packages.

For both the AMBER and DYANA SA/EM structure calculation procedures (see Section 2), the best 45 structures in terms of minimal root mean square (RMS) deviation were selected from the 50 structures periodically chosen in each SA/EM cycle. Fig. 2 shows the corresponding energies and global RMS deviations for both sets of structures. The SA/EM structures from AMBER calculations do always show lower energies and better values of the RMS deviations than the corresponding DYANA SA/EM structures, suggesting a direct influence of the molecular mechanics force field on the results. Fig. 3 shows a superposition of the peptide backbone for the 45 best structures of OFQ2 as obtained from AMBER

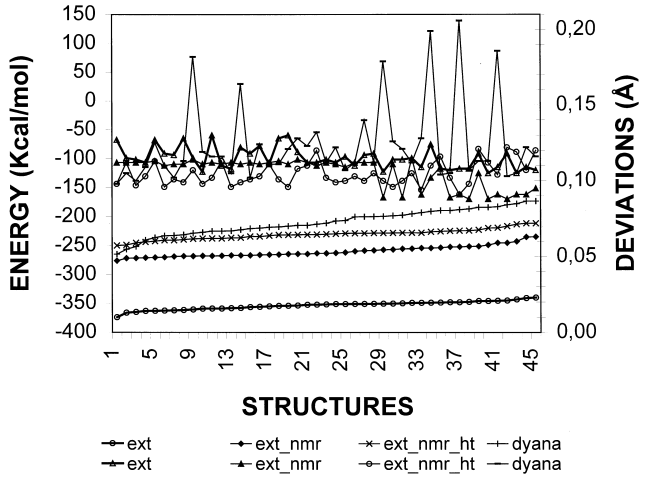

Fig. 2. Energies and global RMS deviations for the best 45 structures of each SA/EM cycle. The following nomenclature was used to designate each SA/EM cycle: **ext** (SA/EM cycle performed with AMBER 5.0, on an initial extended geometry); **ext_nmr** (same as previous but the net charge on charged residue chains is reduced, in this case, to ± 0.2); **ext_nmr_ht** (same as the previous one but the annealing was run at higher temperatures); **dyana** (SA performed with DYANA and EM with AMBER 5.0).

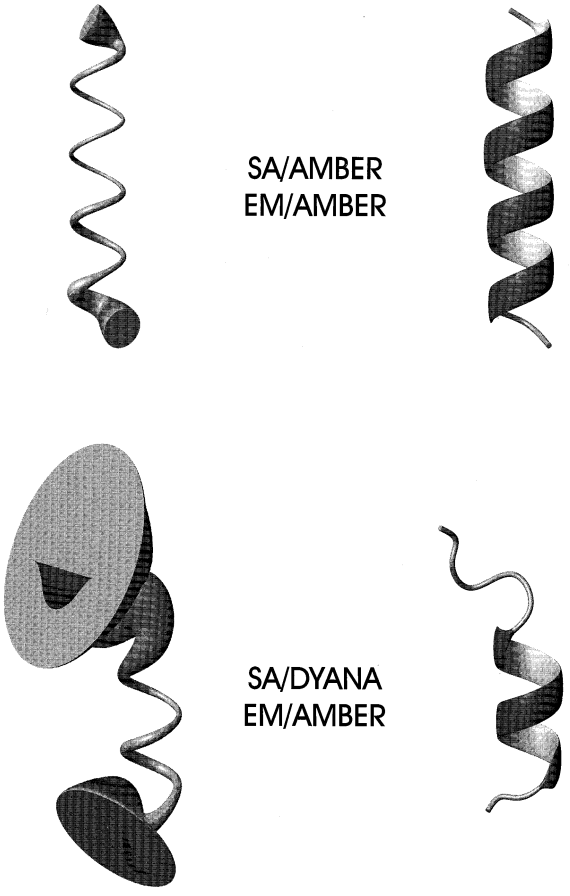

Fig. 3. Cylindrical surrounding of the best structures of OFQ2 obtained from AMBER SA/EM (left upper one) and DYANA SA/AMBER EM (left lower one). 'Cylinders' were obtained by a least square fit of a cylinder surface to the atoms. The 'cylinder radius' is a measure of the global RMS deviation in the corresponding region of the peptide. The right part of the figure shows the corresponding ribbon structures.

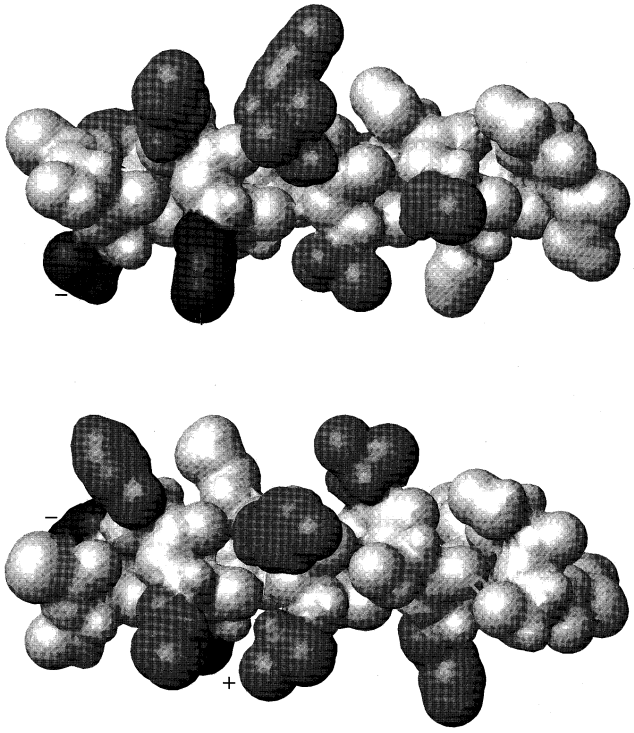

Fig. 4. Different views of OFQ2 (the lower one rotated 90° counterclockwise, around the X axis, in relation to the upper one). The van der Waals surfaces of atoms in side-chains are colored in light gray (hydrophilic residues), dark gray (hydrophobic residues) or black (charged residues; a negative (−) and a positive (+) sign, respectively, are used to label Glu^3 and Arg^6).

SA/EM and DYANA SA/AMBER EM, respectively, where the AMBER structures are those obtained with reduced charges on the ionizable groups. While for the AMBER SA/EM structures, a well defined helical region, ranging from Ser^2 to Ser^{16}, can be observed, the DYANA SA/EM structures do show an helical structure only from Met^5 to Ser^{16}, leaving the N-terminal tetrapeptide out of the helix. In fact, the NMR experimental support for a helical structure, i.e. the presence of medium-range interresidue NOEs, is only observed from Met^5 onwards.

The observation of a shorter helix length and larger deviations from an ideal helix in the structures derived from DYANA SA calculations could be ascribed to:

1. A net attenuation of all the observed NOESY cross-peak intensities, due to instrumental and/or experimental features. If such is the case, DYANA SA would lead to larger variations for the complete peptide due to the scarcity of constraints in some regions of the peptide (i.e. from Phe^1 to Met^5); AMBER force field, on the other hand, could be able to construct a larger helix starting from a well defined helical nucleus.
2. A conformational equilibrium between all-helical and partially helical structures. DYANA SA protocol, which works in a straightforward manner when the set of constraints is complete, would give a description of this conformational equilibrium, whereas AMBER force field would lead in any case to an all-helical structure.

Fig. 4 presents a plot of two views of OFQ2 with hydro-

phobic and hydrophilic residues in different shades of gray. As can be seen from this figure, hydrophobic residues do not cluster according to any known motif (amphiphilic helix, Leu-zipper, coiled-coil) but are irregularly scattered along the helix surface, forming one larger and two smaller hydrophobic pockets. This feature could explain the lack of structure for the peptide when the spectra were run in solvent mixtures different from the helix-promoting mixture HFA/water.

In our previous works [23] on short to medium-sized peptides, the onset of helical structures in solvents with lower structure-promoting ability than HFA/water mixtures is systematically associated with the presence of well defined patterns in the distribution of hydrophobic residues. In this respect, HFA/water could protect the helix from a solvent disruptive effect derived from unfavorable solvation of hydrophobic groups, thus 'restoring' the helical propensity of the peptide emerging from structure prediction calculation and molecular mechanics in vacuum.

This distribution of hydrophobic residues in OFQ2 could suggest close interaction of this peptide with a hydrophobic core or, at least, complementary hydrophobic regions in the intact precursor of the peptide.

4. Discussion

The role of OFQ2 in the control of pain is not yet established with certainty, but a comparison of its primary and secondary structure with those of other 'pain peptides' may help to clarify the issue. OFQ2 shares some sequence similarity with NC in the N-terminal sequence, Phe-Ser-Glu-Phe versus Phe-Gly-Gly-Phe, and with dynorphin A for the presence of Phe in position four. Aromatic residues (Phe and Tyr) in the N-terminal sequence of opioid and ORL1 peptides play a major role in receptor binding and receptor activation [5,24]. Otherwise, there is little sequence similarity, e.g. dynorphin A and NC owe their selectivity to the presence of several cationic residues in the address domain, whereas OFQ2 has but one cationic residue (Arg) in position six. It has been reported that these cationic residues are important requirements for selective receptor binding. The potent analgesic activity of OFQ2 both spinally and supraspinally, not mediated by opioid receptors (μ, δ, κ and ORL1), hints that this new peptide could interact with different receptors or according to Pasternak et al. [10] it may activate downstream naloxone-sensitive opioid mechanisms. Our structural data show that the uniform distribution of hydrophobic residues along the helix is consistent with the presence of a uniformly apolar environment in vivo, such as that of the lipid phase of membranes that hosts the transmembrane helices of ORL1 and opioid receptors. It is tempting to suggest that OFQ2 interacts with the transmembrane helices of a receptor of this kind in a fashion similar to that proposed for β-endorphin [22].

References

[1] Meunier, J.C., Mollerau, C., Toll, L., Suaudeau, C., Moisand, C., Alvinerie, P., Butuour, J.L., Guillemot, J.C., Ferrara, P., Monsarrat, B., Mazargull, H., Vassart, G., Parmentier, M. and Costentin, J. (1995) Nature 377, 532–535.
[2] Reinscheid, R.K., Nothacker, H.P., Bourson, A., Ardati, A., Henningsen, R.A., Bunzow, J.R., Grandy, D.K., Langen, H., Monsma Jr., F.J. and Civelli, O. (1995) Science 270, 792–794.
[3] Okuda-Ashitaka, E., Toshiaki, M., Tachibana, S., Yoshihara, Y., Nishiuchi, Y., Kimura, T. and Ito, S. (1998) Nature 392, 286–289.
[4] Spadaccini, R., Crescenzi, O., Picone, D., Tancredi, T. and Temussi, P.A. (1998) J. Pept. Sci. 5, 306–312.
[5] Salvadori, S., Picone, D., Tancredi, T., Guerrini, R., Spadaccini, R., Lazarus, L.H., Regoli, D. and Temussi, P.A. (1997) Biochem. Biophys. Res. Commun. 233, 640–643.
[6] Crescenzi, O., Guerrini, R., Picone, D., Salvadori, S., Tancredi, T. and Temussi, P.A. (2000) Biopolymers 53, 257–264.
[7] Meunier, J.C. (1997) Eur. J. Pharmacol. 340, 1–15.
[8] Nicholson, J.R., Paterson, S.J., Menzies, J.R.W., Corbett, A.D. and McKnight, A.T. (1998) Can. J. Physiol. Pharmacol. 76, 304–313.
[9] Mogil, J.S., Grisel, J.E., Reinsheid, R.K., Civelli, O., Belknap, J.K. and Grandy, D.K. (1996) Neuroscience 75, 333–337.
[10] Rossi, G.C., Mathis, J.P. and Pasternak, G.W. (1998) Neuroreport 9, 1165–1168.
[11] Florin, S., Leblond, F., Suaudeau, C., Meunier, J.C. and Costentin, J. (1999) Life Sci. 65, 2727–2733.
[12] Atherton, E. and Sheppard, R.C. (1989) in: Solid Phase Peptide Synthesis, pp. 25–53, IRL Oxford University Press, Oxford.
[13] Griesinger, C., Otting, G., Wüthrich, K. and Ernst, R.R. (1998) J. Am. Chem. Soc. 110, 7870–7872.
[14] Jeener, J., Meyer, B.H., Bachman, P. and Ernst, R.R. (1979) J. Chem. Phys. 71, 4546–4553.
[15] Marion, D. and Wüthrich, K. (1983) Biochem. Biophys. Res. Commun. 113, 967–971.
[16] Johnson, B.A. and Blevins, R.A. (1994) J. Biomol. NMR 4, 603–614.
[17] Güntert, P., Mumenthaler, C. and Wüthrich, K. (1997) J. Mol. Biol. 273, 283–298.
[18] Pearlman, D.A., Case, D.A., Caldwell, J.W., Ross, W.S., Cheatham III, T.E., DeBolt, S., Ferguson, D., Seibel, G. and Kollman, P.A. (1995) Comp. Phys. Commun. 91, 1–41.
[19] Koradi, R., Billeter, M. and Wüthrich, K. (1996) J. Mol. Graph. 14, 51–55.
[20] Reymond, M.T., Huo, S., Duggan, B., Wright, P.E. and Dyson, H.J. (1997) Biochemistry 36, 5234–5244.
[21] Rajan, R., Awasthi, S.K., Bhattachajya, S. and Balaram, P. (1997) Biopolymers 42, 125–128.
[22] Saviano, G., Crescenzi, O., Picone, D., Temussi, P.A. and Tancredi, T. (1999) J. Pept. Sci. 5, 410–422.
[23] Amodeo, P., Motta, A., Strazzullo, G. and Castiglione Morelli, M.A. (1999) J. Biomol. NMR 13, 161–174.
[24] Guerrini, R., Rizzi, A., Bianchi, C., Lazarus, L.H., Salvadori, S., Temussi, P.A. and Regoli, D. (1997) J. Med. Chem. 40, 1789–1793.